Eur Biophys J (1997) 25: 431–435

ARTICLE

G. Flood · A. J. Rowe · D. R. Critchley · W. B. Gratzer

Further analysis of the role of spectrin repeat motifs in α-actinin dimer formation

Accepted: 7 November 1996

Abstract Protein constructs consisting of repeats 1–4, repeats 1–3 and repeats 2–4 of the rod domain of chicken α-actinin were expressed as fusion proteins in *Escherichia coli*. Based on the evidence of circular dichroism spectra and cooperative thermal unfolding profiles both truncated rod fragments were judged to have assumed the native structural fold. The thermal stabilities were in both cases significantly lower than that of the intact rod (repeats 1–4). Analyses by sedimentation equilibrium and velocity provided further evidence to show that fragment 1–4 is entirely dimeric in the concentration range of these experiments, resembling therefore the rod domain isolated by proteolytic digestion of native α-actinin. Fragment 2–4, and probably also 1–3, show concentration-dependent association, with dissociation constants, estimated by sedimentation equilibrium, in the 1–10 μM range. Thus, in confirmation of earlier work, all four repeats are required to generate a maximally stable anti-parallel dimer (K_d ~10 pM), suggesting the presence of binding sites in all of them to allow for aligned pairing.

Key words α-actinin · Spectrin-like repeats · Dimer formation

Introduction

α-Actinin belongs to a family of cytoskeletal proteins which also includes spectrin (Speicher and Marchesi 1984), first identified as the major structural component of the erythrocyte cytoskeleton, and dystrophin (Davison and Critchley 1989), the absence of which causes the disease Duchenne muscular dystrophy. α-Actinin is an actin-binding and cross-linking protein and occurs as an antiparallel homodimer. The protein is made up of three domains; an N-terminal actin-binding domain, four spectrin-like repeat units, each of 114 amino acids, and a C-terminal region containing two EF-hand calcium-binding motifs. There are multiple tissue-specific isoforms, each with a subunit molecular mass of approximately 100 kDa. A major functional difference between the muscle and the non-muscle isoforms is that only the latter is calcium sensitive in respect of actin-binding (Blanchard et al. 1989). This difference results from alternative splicing of an exon encoding a region of the first EF-hand motif in the non-muscle isoform. However the calcium-sensitivity is evidently less pronounced in some non-muscle isoforms than in others (Imamura and Masaki 1992). Functional regulation is also exerted by phosphatidylinositol-4,5-bisphosphate (PIP_2) (Fukami et al. 1992), which co-purifies with skeletal muscle α-actinin. Smooth muscle α-actinin is extracted with relatively little bound PIP_2 and has a lower actin-binding affinity, but on addition of exogenous PIP_2 the affinity approaches that of skeletal muscle α-actinin.

Chymotryptic cleavage of chicken gizzard α-actinin liberates a rod-shaped 55 kDa homodimer which encompasses the four internal repeat motifs (Imamura et al. 1988). This dimer was shown to be extremely stable, with an association constant not less than 10^{11} M^{-1}, dissociation being detectable only under denaturing conditions (Kahana and Gratzer 1991). This suggests that formation of the anti-parallel dimer in α-actinin is a function solely of the spectrin-like repeats.

The crystal structure of a single repeat of *Drosophila* α-spectrin shows it to consist of a bundle of three helices (Yan et al. 1993). This structure has since been shown by NMR to apply equally to a single repeat of chicken brain α-spectrin (Pascual et al. 1996). Yan et al. (1993) also give a model for the disposition of successive repeats along the polypeptide chain, in which one long α-helix forms part of two contiguous three-helix bundles. The boundaries of the repeats have been established for spectrin (Winograd et al. 1991), dystrophin (Kahana et al. 1994) and α-actinin (Gilmore et al. 1994). Image reconstruction from two-dimensional crystals of the chicken smooth muscle α-ac-

G. Flood · A. J. Rowe · D. R. Critchley (✉)
Department of Biochemistry, University of Leicester,
University Road, Leicester LE1 7RH, UK (Fax: +44116-2525260)

W. B. Gratzer
MRC Muscle and Cell Motility Unit, King's College London,
26–29 Drury Lane, London WC2B 5RL, UK

tinin dimer led to a staggered model, in which repeats 2, 3 and 4 were paired with repeats 4, 3 and 2 respectively of the antiparallel partner subunit, and repeat 1 was aligned with the actin-binding domain of the other subunit (Taylor and Taylor 1993). Such a model implies that only repeats 2–4 are necessary for rod domain dimer formation, since repeat 1 would remain unpaired. To investigate this hypothesis deletion mutants have been constructed lacking either of the terminal repeats (1 and 4), and dimer formation investigated using analytical ultracentrifugation (Flood et al. 1995). This study strongly suggested that the staggered model was untenable. An aligned, rather than a staggered model was proposed (Flood et al. 1995). We now present a further study of this problem using thermal melting profiles and sedimentation velocity experiments, together with a more rigorous analysis of sedimentation equilibrium experiments.

Materials and methods

cDNAs encoding chicken smooth muscle α-actinin repeats 1–4, 1–3 and 2–4 were generated and subcloned into pGEX-2T or 3X as described previously (Flood et al. 1995). These fragments were then expressed and purified essentially as described by Smith and Johnson (1988).

Circular dichroism was measured in a Jobin-Yvon CD6 instrument in a pathlength of 0.2 or 0.5 mm. For thermal denaturation profiles the temperature was varied between 5 and 70 °C in steps of 5 °C.

Sedimentation equilibrium and velocity measurements were performed in a Beckman Optima XL-A analytical ultracentrifuge with absorption optics. Protein concentrations were determined spectrophotometrically, using molar absorptivities at 280 nm, calculated from the composition (Perkins 1986). The solution columns were scanned at wavelengths between 220 and 280 nm. For sedimentation equilibrium a solution of 1.2 mm column height was centrifuged to equilibrium at 10,000 r.p.m. for 11 hours at 5 °C. The solvent was 100 to 150 mM NaCl containing 1 to 2.5 mM $CaCl_2$, pH 7.5. Plots of absorbance against distance from the rotation centre were fitted to a single-term sedimentation equilibrium relation, corresponding to a non-linear least-squares fit, to yield apparent weight-average molecular weights. Curves were also fitted to a monomer-dimer equilibrium to obtain association constants where appropriate. Average dissociation constants were calculated by fitting experimental data to the equation:

$$M_w = M_1/c\left(2c + \left(K_d - \sqrt{K_d^2 + 8K_d c}\right)\right) \quad (1)$$

where M_w is weight-average molecular mass, M_1 is monomer mass, c is the molar concentration and K_d is the dissociation constant. For sedimentation velocity a solution column of 12 mm was centrifuged at 40,000 r.p.m. for 11 h at 5 °C. Scans were performed at 30-minute intervals. Concentrations were corrected for radial dilution and sedimentation coefficients were calculated by measuring the rate of movement of the point of inflection, which was taken to be the mid-point of the sedimenting boundary for symmetrical traces. Dissociation constants were also estimated when appropriate by comparing calculated plots of sedimentation coefficient against concentration for selected values of the dissociation constant with experimental data.

Results

As described previously (Flood et al. 1995), α-actinin fragments can be successfully expressed in *Escherichia coli* as soluble glutathione S-transferase (GST)-fusion proteins, and liberated from the purified fusion protein by proteolytic cleavage. The α-actinin polypeptides are >90% pure as assessed by SDS-PAGE. The ability of rod fragments to enter the native fold has been assessed for α-spectrin, dystrophin and α-actinin in terms of the α-helicity. The CD spectra of all the expressed α-actinin fragments were characteristic of proteins with a high α-helical content (Table 1) and similar to proteolytically liberated native chicken smooth muscle α-actinin rod (Imamura et al. 1988), indicating correctly folded polypeptides.

Thermal denaturation profiles were measured for the product to allow comparison of the structural stabilities of the repeat combinations (Fig. 1). All fragments displayed

Table 1 Molar residue ellipticities of expressed α-actinin fragments at 222 nm[a]

Fragment	Molar residue ellipticity at 222 nm[b]	Helix content[c]
Repeats 1–4	–23,800	66
Repeats 1–3	–24,800	69
Repeats 2–4	–24,900	69

[a] Measured at 20 °C.
[b] deg cm^2 $dmol^{-1}$.
[c] Approximate α-helicity taking a value of –36,000 deg cm^2 $dmol^{-1}$ for 100% α-helix (Greenford and Fasman, 1969).

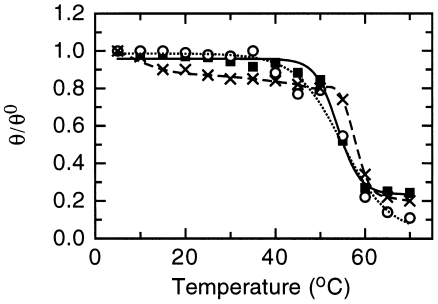

Fig. 1 Thermal denaturation profiles of expressed α-actinin rod fragments, determined by circular dichroism. (Unfolding is measured by the ellipticity at 222 nm relative to that at 5 °C): (×, ---) fragment 1–4; (○, …) fragment 1–3; (■, —) fragment 2–4

sigmoidal transitions but the truncated rods had decreased thermal stability compared to the intact rod. The gradual linear change in ellipticity above the transition region was probably a reflection of the presence of traces of incompletely folded or aggregated material.

To investigate the self-association of the expressed α-actinin fragments, sedimentation equilibrium and velocity measurements were performed. Sedimentation equilibrium revealed that the intact rod preparations were almost entirely dimeric, as reflected by the weight-average molecular masses (Fig. 2A). The data show no significant dependence of molecular mass on concentration. For a species of the size and shape of the α-actinin dimer, we have computed the expected second virial coefficient term (BM), from the sum of the contributions of the excluded volume term, for a particle approximated by a pair of ellipsoids (Rallison and Harding 1984) of axial ratios 12:2:1 (calculated from rotary shadowed images, Flood et al. 1995), and the charge term (Z), at pH 7.5 and ionic strength 0.1 M, given by $Z^2/4$ mM^2 (where m is the ionic strength of the solvent and M the molecular weight of the macromolecule), giving a total of 35 ml/g. A theoretical plot based upon this value is shown in Fig. 2A. The experimental results do not differ significantly from this. Whilst a very weak further interaction between dimer molecules (which would act in opposition to the BM term) cannot be excluded, the experimental data do not offer any support for such a hypothesis.

According to sedimentation equilibrium analysis, both truncated rod fragments, 1–3 and 2–4, showed concentration-dependent association. However, fragment 2–4 indicated the presence of heavy aggregates towards the solution bottom, and therefore the analysis was confined to the upper part. Over a wide range of initial protein concentrations the equilibrium distributions for fragment 1–3 and for the upper part of the solution column of fragment 2–4 were satisfactorily fitted by a monomer-dimer equilibrium model with dissociation constants in the range 0.3–3.8 and 2.0–11.5 µM respectively. In addition we fitted the weight-average molecular masses obtained in these experiments to a monomer-dimer equilibrium, according to Eq. (1), based on the theoretical value of the monomer molecular mass. Figure 2 shows the best fits, which correspond to dissociation constants of 2.0 µM for fragment 1–3 and 6.6 µM for 2–4. These are in reasonable agreement with the results from the individual sedimentation equilibria, and confirm the validity of the monomer-dimer model.

Sedimentation velocity experiments were performed on the expressed polypeptides and sedimentation coefficients obtained as a function of concentration. The observed sedimentation coefficients were corrected to standard conditions of water at 20 °C. The intact rod made up of repeats 1–4 showed a small increase in apparent sedimentation coefficient, with diminishing cconcentration, characteristic of non-associating systems. By contrast, the fragments comprising repeats 1–3 and 2–4 both displayed an increase in sedimentation coefficient with increasing concentration, indicative as before of self-association. An estimate of the association constant, assuming a rapid

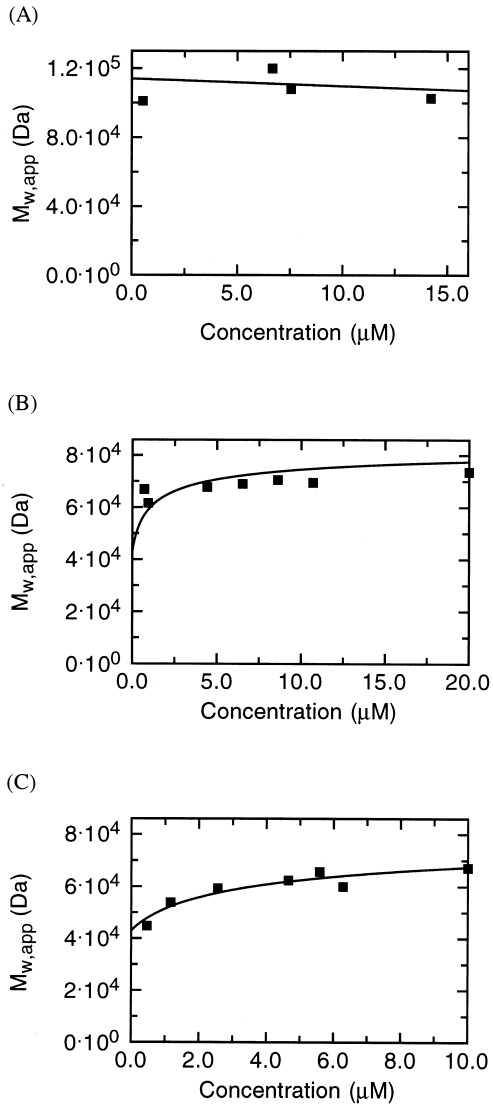

Fig. 2 **A** Concentration-dependence of apparent weight-average molecular mass for fragment 1–4. **B** Concentration-dependence of apparent weight-average molecular mass for fragment 1–3. The curve is based on Eq. (1), fixing the monomer mass at the theoretical value. Each experimental point is derived from a sedimentation equilibrium experiment, in which the distribution in all cases conforms satisfactorily to a monomer-dimer equilibrium with dissociation constants of 0.3–3.8 µM. The *curve* shown corresponds to a dissociation constant of 2.0 µM. **C** Concentration-dependence of weight-average molecular mass for fragment 2–4. The same procedure was followed as in **B**. The curve of best fit corresponds to a dissociation constant of 6.6 µM

monomer-dimer equilibrium, can then be made, based on the procedure of Gilbert and Gilbert (1973), as modified by Emes and Rowe (1978). It is first necessary to know the concentration-dependence of the sedimentation coefficients of the monomer and dimer, which is assumed to be linear with a proportionality constant, k_s. This is given by $k_s = 2\bar{v}\,((V_s/\bar{v})+(f/f_0)^3)$ where $\bar{v}$ is the partial specific volume of the particle, V_s the corresponding hydrated volume and (f/f_0) the frictional ratio (Emes and Rowe 1978). A value of 0.3 g/g is assumed for the hydration. Plots of

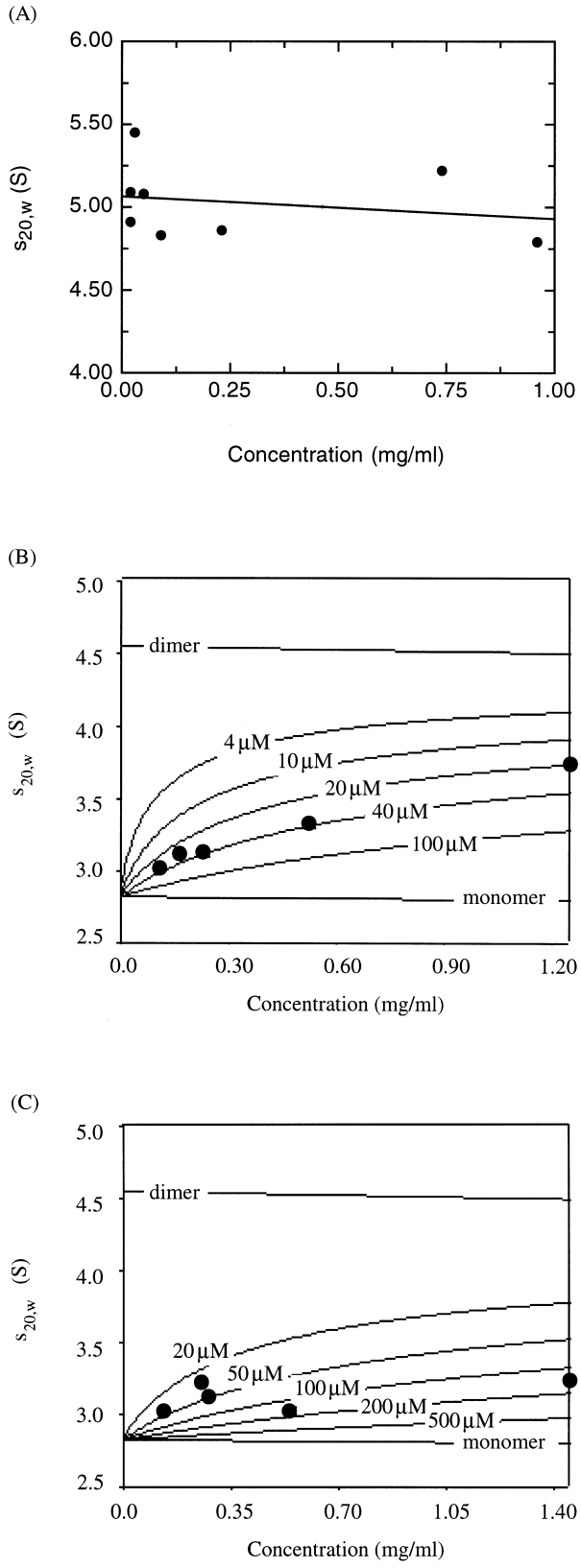

Fig. 3 Concentration dependence of sedimentation coefficient for (**A**) fragments 1–4, (**B**) 1–3 and (**C**) 2–4. The *curves* are calculated for the indicated dimer dissociation constants, and the points are experimental values, yielding apparent dissociation constants of 40 μM and 100 μM

weight-average sedimentation coefficient against protein concentration are then constructed for a series of values of the dimer dissociation constant, K_d, and a match to the experimental data is sought. The best fit (Fig. 3) for fragment 1–3 gave a value of ca. 40 μM and that for fragment 2–4 μM. These values are larger than those obtained by sedimentation equilibrium, but the method suffers from several drawbacks, in particular that protein association reactions are in general accompanied by a significant volume increase and are consequently strongly pressure-dependent. Perturbation of the equilibrium by hydrostatic pressure down the liquid column is therefore inescapable (Harrington and Kegeles 1973). Assuming that the volume change accompanying the self-association of our α-actinin fragments are the same, our results nevertheless confirm not only that both undergo self-association within the concentration range of these experiments, but also that the propensity of fragment 1–3 to self-associate is stronger than that of fragment 2–4.

Discussion

The thermal denaturation profiles establish that the bulk of both expressed polypeptide preparations attained their native fold, although a small proportion of unfolded material generally remained, as indicated by the small change in ellipticity in the temperature range below the transition. Rapid spontaneous refolding has been similarly demonstrated for single repeating units from spectrin (Winograd et al. 1991), dystrophin (Kahana and Gratzer 1995) and α-actinin (Gilmore et al. 1994). The sharp conformational transitions displayed by the two three-fragments studied here imply considerable long-range cooperativity of melting along the rod.

The thermal stabilities of both fragments are, however, lower than that of the intact rod domain of four residues (Flood et al. 1995). Whether this is a consequence of an increase in the length of the cooperative unit in the latter or of its much stronger self-association, with $K_d < 10$ pM (Kahana and Gratzer 1991), is not yet clear. Certainly the free energy of dimerisation of the native structure would be reflected in the thermal stability of its conformation. In the case of the three-repeat fragments, the stabilisation expected to result from dimerisation can in principle be readily calculated, if the melted form does not self-associate. In the concentration range of our circular dichroism measurements, with a dimer dissociation constant of say 5 μM (almost certainly a considerable underestimate) at the transition mid-point (50–55 °C), a stabilisation of no more than 2–3 °C is predicted.

The results now obtained by sedimentation velocity analysis, and also by further interpretation of sedimentation equilibrium data, are consistent with both the thermal melting data currently presented, and with an earlier hypothesis (Flood et al. 1995). This argues strongly against a staggered model for the dimer, in which there are only three pairwise interactions between the repeats in the con-

stituent chains, while terminal repeat 1 or 4 pairs with the non-homologous actin-binding domain as partner (Taylor and Taylor 1993). The extreme stability of the dimer formed by the isolated rod domain (Imamura et al. 1988; Kahana and Gratzer 1991) in fact renders it unlikely that either the actin-binding domain or the EF-hand domain play any important part in stabilising the α-actinin dimer. Viel and Branton (1994) found that sequences adjoining the four complementary terminal domains of *Drosophila* spectrin contributed to dimer formation, but this was not confirmed in studies on the analogous human erythroid spectrin system (Ursitti et al. 1996). The implication of our results then is that pairwise interactions between all four aligned repeats in the antiparallel orientation contribute to the stability of the dimer.

Speicher et al. (1992) have shown that the formation of the antiparallel heterodimer of erythroid spectrin is dependent on pairing of the first four complete repeats at the N-terminal end of the β-chain (β1–β4) with the last four repeats of the α-chain (α18–α21). A characteristic of these strongly associating repeats, shared by their counterparts in *Drosophila* spectrin (Viel and Branton 1994), is that they all contain an eight-residue insert at their N-terminal ends. Excision of these segments from the sequence resulted in a gross loss in the capacity to associate. Thus for example, the elimination of such an eight-residue insert from β1 of a human erythroid spectrin construct led to a tenfold decrease in affinity of binding to the complementary subunit (Ursitti et al. 1996). The four α-actinin rod repeats display the highest homology (29–47% identity) with the strongly associating spectrin repeats and indeed all contain N-terminal eight-residue inserts. The phasing selected for the truncated rod fragments used here incorporated the eight-residue inserts. Whether these serve the surmised function of stabilising the dimer α-actinin will be determined by the examination of further constructs.

Acknowledgements This work was supported in part by a Cancer Research Campaign grant to D.R.C., a Muscular Dystrophy Group grant to W.B.G. and a BBSRC grant to A.J.R. in support of the National Centre for Macromolecular Hydrodynamics. G.F. was supported by a University of Leicester research studentship.

References

Blanchard A, Ohanian V, Critchley DR (1989) The structure and function of α-actinin. J Muscle Res Cell Motil 10:280–289

Davison MD, Critchley DR (1988) α-Actinins and DMD protein contain spectrin-like repeats. Cell 52:159–160

Emes CH, Rowe AJ (1978) Hydrodynamic studies on the self association of vertebrate skeletal muscle myosin. Biochem Biophys Acta 537:110–124

Flood G, Kahana E, Gilmore AP, Rowe AJ, Gratzer WB, Critchley DR (1995) Association of structural repeats in the α-actinin rod domain. Alignment of inter-subunit interactions. J Mol Biol 252:227–234

Fukami K, Furuhashi K, Inagaki M, Endo T, Hatano S, Takenawa T (1992) Requirement of phosphatidylinositol 4,5-bisphosphate for α-actinin function. Nature 359:150–152

Gilbert LM, Gilbert GA (1973) Sedimentation velocity measurement of protein association. In: Hirs CHW, Timasheff SN (eds) Methods in enzymology, vol 27. Academic Press, New York, pp 273–296

Gilmore AP, Parr T, Patel B, Gratzer WB, Critchley DR (1994) Analysis of the phasing of the four spectrin-like repeats in α-actinin. Eur J Biochem 225:235–242

Greenfield N, Fasman GD (1969) Computed circular dichroism spectra for the evaluation of protein conformation. Biochemistry 8:4108–4114

Harrington WF, Kegeles G (1973) Pressure effects in ultracentrifugation of interacting systems. In: Hirs CHW, Timasheff SN (eds) Methods in enzymology, vol 27. Academic Press, New York, pp 306–345

Imamura M, Endo T, Kuroda M, Tanaka T, Masaki T (1988) Substructure and higher structure of chicken smooth muscle α-actinin molecule. J Biol Chem 263:7800–7805

Imamura M, Masaki T (1992) A novel non-muscle α-actinin: purification and characterisation of chicken lung α-actinin. J Biol Chem 267:25927–25933

Kahana E, Gratzer WB (1991) Properties of the spectrin-like element of smooth-muscle α-actinin. Cell Motil Cytoskel 20:242–248

Kahana E, Marsh PJ, Henry AJ, Way M, Gratzer WB (1994) Conformation and phasing of dystrophin structural repeats. J Mol Biol 235:1271–1277

Kahana E, Gratzer WB (1995) Minimum folding unit of dystrophin rod domain. Biochemistry 34:8110–8114

Pascual J, Pfuhl M, Rivas G, Pastore A, Saraste M (1996) The spectrin repeat folds into a three-helix bundle in solution. FEBS Lett 383:201–207

Perkins SJ (1986) Protein volumes and hydration effects. The calculation of partial specific volumes, neutron scattering matchpoints and 280-nm absorption coefficients for proteins and glycoproteins from amino acid sequences. Eur J Biochem 157:169–180

Rallison JM, Harding SE (1985) Excluded volume for pairs of triaxial ellipsoids at dominant brownian motion. J Colloid Interface Sci 103:284–289

Smith DB, Johnson KS (1988) Single step purification of proteins expressed in *E. coli* as fusion proteins with glutathione-S-transferase. Gene 67:31–40

Speicher DW, Weglarz L, DeSilva TM (1992) Properties of human red cell spectrin heterodimer (side-to-side) assembly and identification of an essential nucleation site. J Biol Chem 267:14775–14782

Speicher DW, Marchesi VT (1984) Erythrocyte spectrin is comprised of many homologous triple helical segments. Nature 311:177–180

Taylor KA, Taylor DW (1993) Projection image of smooth muscle α-actinin from two-dimensional crystals formed on positively charged lipid layers. J Mol Biol 230:196–205

Ursitti JA, Kotula L, DeSilva TM, Curtis PJ, Speicher DW (1996) Mapping the human erythrocyte β-spectrin dimer initiation site using recombinant peptides and correlation of its phasing with the α-actinin dimer site. J Biol Chem 271:6636–6644

Viel A, Branton D (1994) Interchain binding at the tail end of the *Drosophila* spectrin molecule. Proc Natl Acad Sci USA 91: 10839–10843

Winograd E, Hume D, Branton D (1991) Phasing the conformational unit of spectrin. Proc Natl Acad Sci USA 88:10788–10791

Yan Y, Winograd E, Viel A, Cronin T, Harrison SC, Branton D (1993) Crystal structure of the repetitive segments of spectrin. Science 262:2027–2030